

Insight of Natural Compounds Halimane Diterpenoids against *Mycobacterium tuberculosis*: Virtual Screening, DFT, Drug-Likeness, and Molecular Dynamics Approach

Laurent Gael Eyia Andiga¹, Boris Davy Bekono^{2,3*} , Désiré Mama Bikele^{1*} ,
Pie Pascal Onguéné Amoa^{3,4} , Luc Calvin Owono Owono^{2,5}, Luc Léonard Mbaze Meva'a¹

¹Department of Chemistry, Faculty of Science, University of Douala, Douala, Cameroon

²Department of Physics, Ecole Normale Supérieure, University of Yaoundé 1, Yaoundé, Cameroon

³Center for Drug Discovery, Faculty of Science, University of Buea, Buea, Cameroon

⁴Department of Chemistry, University of Yaoundé I Institute of Wood Technology, Mbalmayo, Cameroon

⁵CEPAMOQ, Faculty of Science, University of Douala, Douala, Cameroon

Email: *boris.bekono@univ-yaounde1.cm, *bikelemama@yahoo.fr

How to cite this paper: Andiga, L.G.E., Bekono, B.D., Bikele, D.M., Amoa, P.P.O., Owono, L.C.O. and Meva'a, L.L.M. (2024) Insight of Natural Compounds Halimane Diterpenoids against *Mycobacterium tuberculosis*: Virtual Screening, DFT, Drug-Likeness, and Molecular Dynamics Approach. *Computational Molecular Bioscience*, 14, 35-58.

<https://doi.org/10.4236/cmb.2024.142003>

Received: February 17, 2024

Accepted: May 5, 2024

Published: May 8, 2024

Copyright © 2024 by author(s) and Scientific Research Publishing Inc. This work is licensed under the Creative Commons Attribution International License (CC BY 4.0).

<http://creativecommons.org/licenses/by/4.0/>



Open Access

Abstract

In the purpose to design novel antituberculosis (anti-TB) drugs agents against *Mycobacterium tuberculosis* (Mtb), we have built a molecular library around 42 Halimane Diterpenoids isolated from natural sources. Two Mtb enzymes drug targets (Mtb *Mycothioli S-transferase* and Mtb *Homoserine transacetylase*) have been adopted. The pharmacological potential was investigated through molecular docking, molecular dynamics simulation, density functional theory (gas phase and water) and ADMET analysis. Our results indicate that (2R,5R,6S)-1,2,3,4,5,6,7,8-octahydro-5-((E)-5-hydroxy-3-methylpent-3-enyl)-1,1,5,6-tetramethylnaphtha-lene-2-ol (compound 20) has displays higher docking score with each of the selected drug targets. In addition, this molecule exhibits a satisfactory drug potential activity and a good chemical reactivity. Its improved kinetic stability in the Mtb *Mycothioli S-transferase* enzyme reflects its suitability as a novel inhibitor of Mtb growth. This molecule has displayed a good absorption potential. Our results also show that its passive passage of the intestinal permeability barrier is more effective than that of first-line treatments (ethambutol, isoniazid). In the same way, this anti-TB druglikeness has shown to be able to cross the blood brain barrier.

Keywords

Antituberculosis Druglikeness, Density Functional Theory, Halimane Diterpenoids, Molecular Docking, Molecular Dynamics Simulation

1. Introduction

Diseases are nowadays one of the major problems facing world populations in general and those in sub-Saharan Africa in particular [1] [2]. To cope with diseases, more often chemical entities are used. Thus, several chemical entities have been discovered as drugs and are grouped into different categories based on their actions on the disease. Among them are antibiotics and anti-inflammatories [3] [4] [5]. Unfortunately, these drugs often date back many years, and as a result, resistance has been developed by pathogens that cause diseases. This is currently a major public health concern that needs to be taken into consideration by both governments and researchers [6] [7]. The most promising approach to fighting with these resistances is the more than urgent development of new therapeutic formulas. These new drugs must interact with well-known target proteins as well as the search for new targets that might lead to new successful therapies [8] [9]. Tuberculosis (TB) is a highly contagious disease after COVID-19 caused by *Mycobacterium tuberculosis* (Mtb). Immunodepressed patients such as the HIV-positive individuals are more susceptible to TB, and its major concern is due to the high resistance of the bacterium to the available drugs such as isoniazid, rifampicin, etc. [10] [11] [12]. The World Health Organization aims to reduce mortality rates and eradicate TB under 2030 by improving access to interventions [13]. TB is a leading cause of death among infectious diseases worldwide, resulting in a significant global public health burden. In 2022, there were 1.30 million deaths worldwide due to TB, with 1.13 million deaths among HIV-negative individuals and approximately 167,000 deaths among HIV-positive individuals. Although there was a 19% reduction in TB deaths between 2015 and 2022, the TB strategy's goal of a 75% reduction by 2025 was not met [14]. The lungs are affected primarily by Mtb and become active when the immune system weakens. This triggers a fight between the hosts and the pathogen, releasing free radicals (ROS) and survival mechanisms used by Mtb. Patients with TB present more levels of ROS than healthy individuals. Immune response and inflammation keep a significant role in TB disease [15]. TB is a disease that can be treated with antibiotics. Currently active TB is treated with several regimens that can take 4, 6, or 9 months depending on the treatment plan. The available TB treatment regimens include the 4-month Rifapentine-moxifloxacin TB Treatment Regimen and the 6- or 9-month RIPE (rifampicin, isoniazid, pyrazinamide, and ethambutol) TB Treatment Regimen. However, there is a risk of drug resistance [16] [17] [18]. So to combat this, more toxic drugs are available, but they are not easily accessible to those with lower incomes. Additionally, the treatment itself has several unwanted side effects, such as liver toxicity, gastrointestinal issues, skin rashes, eyes problem, and heart complications. It is essential to improve the management of TB patients by reducing these side effects and increasing the effectiveness of the drugs. Despite the increasing worldwide incidence of TB and its alarming threat toward the public health, no novel anti-TB drugs have been introduced into clinical practice over the past decades. The impact of ever-increasing drug resis-

tance, the serious side effects of some current anti-TB drugs, and the lack of efficacy of current treatments in immunodepressed patients combine to make the development of new antimycobacterial agents an urgent priority. One key approach is to combine anti-TB antibiotics with agents that target the antioxidant, which may help to eliminate the disease more quickly. However, research in this area is still in the early stages of evaluation [19]. Previous studies show that the combination of therapeutic supplements such as vitamin C and cysteine has a rapid inhibitory effect on bacteria, preventing their proliferation in the host [20].

This paves the way for research into natural tropical antioxidants that are accessible to all. Research has been carried out on halimane diterpenoids isolated from plant sources (Marchantiophyta, Magnoliophyta) and animal sources (Porifera, Mollusca, Chordata, Cnidaria) showing their potential to inhibit the virulence factors of the Mtb responsible for this disease [21]. Three labdane-type of diterpenoids (18-nor-labd-13(E)-ene-8 α , 15-diol, labd-13(E)-ene-8 α , 15-diol and austroinulin) has been extracted from the stem bark of *Croton Sylvaticus* [22]. From DPPH free radical scavenging, Frum *et al.* have previously described the relevant antioxidant activity of the extract of the stem bark of *Croton Sylvaticus* [23]. Research on the ethnobiological activity on plants shows that South African traditional healers used this plant to treat the TB and mental disorder [24]. These findings are a proof of the double competence of these extracts from the stem bark as a tonic and as a therapeutic agent for TB. In addition, the requirements for the incorporation of diastereomers of the same halimane diterpenoids into other halimane diterpenoids in clearly defined ratios blocks the phagosome maturation and macrophage phagocytosis in human cells [25]. For instance, the compound tuberculosinol can be added in the proportion (1:1) to the mixture of the diastereoisomers isotuberculosinol (R) and isotuberculosinol (S) in turn in the proportion (1:3) [26]. Minor studies on the stereo-clarification of halimane diterpenoids discovered to date have been carried out by Roncero *et al.* [21].

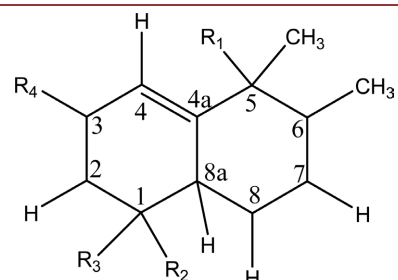
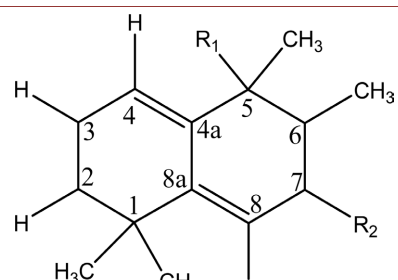
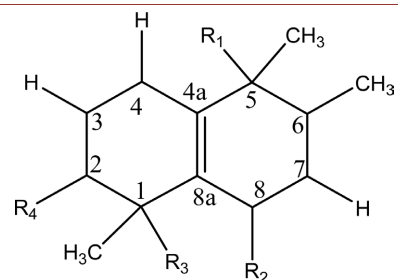
Despite these advances, an analysis of the impact of their biological, pharmacokinetic and medicinal activities is lacking. Among 42 halimane diterpenoids compound selected, we have investigated the better anti-TB druglikeness able to block the development and maturation of the Mtb. Consequently, molecular docking and dynamic simulation have been performed. The pharmacokinetic parameters of this elected anti-TB druglikeness estimated have compare to those of three first-line treatments: ethambutol Isoniazid and amikacin.

2. Materials and Methods

2.1. Ligands Preparation and Selection

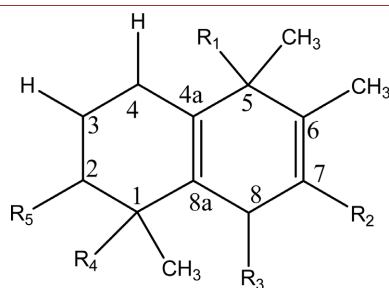
Forty-two (42) halimane diterpenoids compounds of natural origin, as they occur in African flora. The absolute configurations are presented in **Table 1** [21]. They are carried out with under force field in the Open Babel plug-in tool of PyRx 0.8 tool to obtain optimized geometric [27]. After that, they became as

Table 1. Molecular registration and substituent specification.

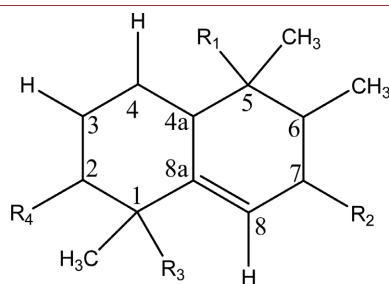
				
N*	R ₁	R ₂	R ₃	R ₄
(1)	CH ₃ -CH ₂ -(CH ₃)C-(O)-CH=CH ₃	COOMe	CH ₃	H
(2)	CH ₂ -CH ₂ -(CH ₃)C(OH)-CH=CH ₂	COOMe	CH ₃	H
(3)	CH ₂ -CH ₂ -C(CH ₃)-CH(OH)-CH ₂ OH	COOH	CH ₃	H
(4)	CH ₂ -CH ₂ -(CH ₃)C(OH)-CH(OAc)-CH ₂ OAc	COOMe	CH ₃	H
(5)	CH ₂ -CH ₂ -(CH ₃)C(OH)-CH=CH ₂	COOH	CH ₃	H
(6)	CH ₂ -CH ₂ -(CH ₃)C(OH)-CH=CH ₂	COOH	CH ₃	OH
(7)	CH ₂ -CH ₂ -(CH ₃)C(OH)-CH=CH ₂	COOH	CH ₃	O
(8)	CH ₂ -CH ₂ -(CH ₃)C=CH-COOH	CH ₃	CH ₂ OH	H
(9)	CH ₂ -CH ₂ -(CH ₃)C=CH-CH ₂ OH	CH ₃	CH ₂ OH	OH
(10)	CH ₂ -CH ₂ -(CH ₂ OH)CH-CH ₂ -CH ₂ OH	CH ₃	CH ₃	H
				
N°	R ₁	R ₂		
(11)	CH ₂ -CH ₂ -(CH ₃)C(OH)-CH=CH ₂	OH		
(12)	CH ₂ -CH ₂ -(CH ₃)C(OH)-CH=CH ₂	OMe		
(13)	CH ₂ -CH ₂ -(CH ₃)C(OH)-CH=CH ₂	OEt		
				
N°	R ₁	R ₂	R ₃	R ₄
(14)	CH ₂ -CH ₂ -(CH ₃)C=CH-CHO	H	CH ₃	OH

Continued

(15)	$\text{CH}_2\text{-CH}_2\text{-(CH}_3\text{)C=CH-COOH}$	H	CH_3	H
(16)	$\text{CH}_2\text{-CH}_2\text{-(CH}_3\text{)C=CH-COOMe}$	H	CH_3	H
(17)	$\text{CH}_2\text{-CH}_2\text{-(CH}_3\text{)C(OH)-CH=CH}_2$	H	CH_3	H
(18)	$\text{CH}_2\text{-CH}_2\text{-(CH}_3\text{)C(OH)-CH=CH}_2$	H	CH_3	OH
(19)	$\text{CH}_2\text{-CH}_2\text{-(CH}_3\text{)CH-CH}_2\text{-COOH}$	H	CH_3	H
(20)	$\text{CH}_2\text{-CH}_2\text{-(CH}_3\text{)C=CH-CH}_2\text{OH}$	H	CH_3	OH
(21)	$\text{CH}_2\text{-CH}_2\text{-(CH}_3\text{)C(OH)-CH=CH}_2$	H	CH_3	OH
(22)	$\text{CH}_2\text{-CH}_2\text{-(CH}_3\text{)C(OH)-CH=CH}_2$	H	CH_2OH	H
(23)	$\text{CH}_2\text{-CH}_2\text{-(CH}_3\text{)C(OH)-CH=CH}_2$	H	CH_3	OAc
(24)	$\text{CH}_2\text{-CH}_2\text{-(CH}_3\text{)C(OH)-CH=CH}_2$	O	CH_2OH	H
(25)	$\text{CH}_2\text{-CH}_2\text{-(CH}_3\text{)C(OH)-CH=CH}_2$	OAc	CH_3	H
(26)	$\text{CH}_2\text{-CH}_2\text{-(CH}_3\text{)C(OH)-CH=CH}_2$	OAc	CH_3	H
(27)	$\text{CH}_2\text{-CH}_2\text{-(CH}_3\text{)C(OH)-CH=CH}_2$	OAc	CH_3	H
(28)	$\text{CH}_2\text{-CH}_2\text{-(CH}_3\text{)C(OH)-CH=CH}_2$	OH	CH_3	H
(29)	$\text{CH}_2\text{-CH}_2\text{-(CH}_3\text{)C(OH)-CH=CH}_2$	OH	CH_3	H
(30)	$\text{CH}_2\text{-CH}_2\text{-(CH}_3\text{)C(OH)-CH=CH}_2$	OMe	CH_3	H
(32)	$\text{CH}_2\text{-CH}_2\text{-(CH}_3\text{)CH-CH}_2\text{-CH}_2\text{OH}$	H	CH_3	OH



N°	R_1	R_2	R_3	R_4	R_5
(25)	$\text{CH}_2\text{-CH}_2\text{-(CH}_3\text{)C(OH)-CH=CH}_2$	OAc	CH_3	CH_3	H
(31)	$\text{CH}_2\text{-CH}_2\text{-(CH}_3\text{)C=CH-CH}_2\text{OH}$	OH	O	CH_2OAc	O



N°	R_1	R_2	R_3	R_4
(33)	$\text{CH(OAc)-CH}_2\text{-(CH}_3\text{)C=CH-COOH}$	H	CH_3	H
(34)	$\text{CH}_2\text{-CH}_2\text{-(CH}_3\text{)CH-CH}_2\text{-COOH}$	H	CH_2OH	H

Continued

(35)	$\text{CH}_2\text{-CH}_2\text{-(CH}_3\text{)CH-CH}_2\text{-COOH}$	H	CH_3	OH
(36)	$\text{CH}_2\text{-CH}_2\text{-(CH}_3\text{)CH-CH}_2\text{-COOH}$	H	CH_2OH	OH
(37)	$\text{CH}_2\text{-CH}_2\text{-(CH}_3\text{)C=CH-CH}_2\text{OH}$	H	CH_3	H
(38)	$\text{CH}_2\text{-CH}_2\text{-(CH}_3\text{)C(OH)-CH=CH}_2$	H	CH_3	H
(39)	$\text{CH}_2\text{-CH}_2\text{-C(CH}_3\text{)-CH=CH}_2$	H	CH_3	H
(40)	$\text{CH}_2\text{-CH}_2\text{-(CH}_3\text{)C(OH)-CH=CH}_2$	H	CH_3	OAc
(41)	$\text{CH}_2\text{-CH}_2\text{-(CH}_3\text{)C(OH)-CH=CH}_2$	O	CH_3	H
(42)	$\text{CH}_2\text{-CH}_2\text{-(CH}_3\text{)C(OH)-CH=CH}_2$	H	CH_3	OH

ligand and automatically converted to pdbqt format.

2.2. Targets Selection and Preparation

Two validated Mtb drug targets namely Homoserine transacetylase (PDB ID 8F2L) and Mycothiol S-transferase enzyme (PDB ID 8F5V) have been selected according to their potential roles in Mtb maturation besides development [28] [29]. Their 3D co-crystallized structures have been retrieved in PDB code with respectively PDB ID 8F2L and 8F5V. Each of the two selected targets has been obtained by X-ray diffractions with resolution 2.89 Å and 1.45 Å respectively.

The two receptors were prepared for docking by removing all water molecules, co-crystallized ligands, cofactor ions, as well as charges and hydrogens using the BIOVIA Discovery Studio 2021 client software [30]. Opened in the PyRx virtual screening tool, everyone is treated as a macromolecule structure and saved in pdbqt format [31].

2.3. Molecular Docking Validation and Study Process

1) Description

In the field of computer-aided drug design, molecular docking is popular technique employed to predict the affinity between the three-dimensional structures of a small molecule (ligand) and a macromolecule (protein). This method uses mathematical algorithms to study the interactions of natural compounds with specific protein targets such as mycobacterial enzymes. It is based on the binding affinity energy of compounds with proteins. The result is the formation of complexes, the most stable of which corresponds to the lowest affinity energy [32] [33].

2) Validation of Docking Protocol

Separation of the co-crystallized ligand from each protein and repetition of the docking studies in the same region with the re-docked nature ligand is a useful way of validating molecular docking. The docking simulations of the orientation and position of the ligands used have been validated by redocking experiments, through a representation of the valid and reasonable potential binding mode of the inhibitors. The molecular structure of halimane derivatives was optimized using the Gaussian 09 and Gauss View 6.0 suite programs, with

density functional theory (DFT) and Becker's three-parameter calculation method (B3) combined with Lee, Yang, and Parr's non-local correlation functional (LYP) and a 6-311++G (d, p) basis set [34] [35] [36] [37] [38]. DFT was chosen as it provides reliable results in predicting molecular geometry and properties, such as total energy and molecular shape [37] [39]. The 6-311++G (d, p) basis set was selected due to its ability to account for diffusion, polarization, and angular flexibility in hydrogen-bonded organic systems [40]. All geometric optimizations were followed by determination of the vibrating frequencies. Before carrying out molecular docking experiments on the Mtb enzymes *Homoserine transacetylase* and *Mycothiol S-transferase*, a protocol was developed to focus on the active site of these enzymes and take into account surrounding amino acid residues. Cofactors, water molecules and co-crystallized ligands were removed from the enzymes. The co-crystallized ligand was docked into the protein structure to determine the best conformation using the calculated RMSD value [41]. Each amino acid residue interacting with the ligand was realigned using PyMol software [42].

Virtual screening was then carried out by converting Mtb ligands and enzyme receptors to PDBQT format using PyRx software [43]. Ligands with the best binding energy and lowest RMSD value were selected. Finally, the hydrogen, hydrophobic and protein-ligand interactions of the best ligands were studied using Discovery Studio [30].

2.4. Pharmacokinetic and Drug-Likeness Study

In the biological system, the pharmacokinetic parameters of candidate therapeutic molecules, such as their ADMET are crucial to the selection of those with drug potential activity. This selection enables the creation and development of new innovative drugs. Availability of a therapeutic compound for administration and absorption in the body is an essential aspect of drug-likeness. It is based on evaluating the most suitable candidates in accordance with the ADMET's rules. Maestro Schrödinger software and the online resource Swiss-ADME were used to perform the ADMET properties of the compounds [44] [45] [46].

2.5. DFT Studies

The electrophilic reactivity and stability of the optimized halimane compounds was classified according to their electrophilicity index (ω). The index was calculated using the following expression in Equation (1).

$$\omega = \mu^2 / 2\eta \quad (1)$$

with the variables μ , η , S , and χ correspond to chemical potential, hardness, global softness, and electronegativity (see Equation (1)). They are determined by expressing the energy of the HOMO and LUMO orbitals using the following formulae [47].

$$\mu = 1/2(E_{\text{HOMO}} + E_{\text{LUMO}}) \quad (2)$$

$$\eta = 1/2(E_{\text{HOMO}} + E_{\text{LUMO}}) \quad (3)$$

$$S = 1/2\eta \quad (4)$$

$$\chi = -\eta \quad (5)$$

2.6. Molecular Dynamics Simulation (MDs)

The MDs is a study conformational changes and the stability of ligand-binding complexes over simulation time. These simulations were conducted using the Desmond simulation package in Schrödinger software, based on two complexes obtained from protein docking [48]. These simulations were performed at standard temperature and pressure, with a 100 ns duration and snapshots recorded every 100 ps. Short-range interactions were analyzed using OPLS4 force field parameters and a cutoff radius of 9.0 Å, while long-range electrostatic interactions were calculated using the Particle-Mesh Ewald approach [49]. The Nose-Hoover and Martyna-Tobias-Klein chain coupling scheme was used for constant temperature and pressure conditions. Water molecules were modeled using a simple point-charge model. This analysis included evaluating factors of root mean square deviation (RMSD) and fluctuation (RMSF), as well as examining ligand contacts with amino acids using the Desmond interaction diagram [50] [51].

2.7. Interaction Energy Calculations

The unbound interactions between the ligand compound and enzyme residues were analyzed using the Discovery Studio software to calculate the interaction energy values [30]. In addition, the molecular modeling interaction values between the ligand compound and enzyme residues in unbound interactions were determined using the same software such describe in our previous work [52] [53]. This study utilized the interaction energy protocol with the CHARMM force field and dielectric constant to identify electrostatic and van der Waals forces [54]. By analyzing the interaction energy contributions per active site residue, the significance of individual interactions was identified and facilitated comparative analysis. This method allows for the selection of affinity values that predict favorable and unfavorable PEP substitutions.

3. Results and Discussion

3.1. Docking Procedure

3.1.1. Validation Protocol

To create a model able to correlate the structure of candidate molecules with their ability to bind to receptor crystal structures (PDB ID: 8F2L and 8F5V) [55]. For each structure, we started by testing a combination of parameters to best reproduce (with high accuracy) the native ligand conformation, in order to create a reliable protocol. In this context, the ligand was removed and then re-docked according to the rigid docking process with the crystal structure. The RMSD obtained between the native ligand and the realigned ligand in Homoserine trans-

acetylase and Mycothiol S-transferase enzyme was respectively 1.326 Å and 3.404 Å.

3.1.2. Molecular Docking Analysis of the Mtb's Protein

Now that the submitted protocol has been validated, candidate molecules are subjected to molecular docking to determine the best binding mode for the ligand-Mtb enzyme protein complex. Each ligand that docked into the binding site of the Mtb protein produced different poses. Molecular docking of 42 halimane diterpenoids produced the highest affinity of ligand for binding to each Mtb enzyme (**Table 2**). Each ligand (target molecule)-protein bond is stable due to this binding affinity. Adjustment of the binding pocket is best when the binding affinity value is negative. For this reason, binding affinity represents a more efficient binding pocket fit [56].

In view of the higher calculated affinity results in complex Homoserine trans-acetylase and its top 5 position in complex Mycothiol S-transferase enzyme, (2R,5R,6S)-1,2,3,4,5,6,7,8-octahydro-5-((E)-5-hydroxy-3-methylpent-3-enyl)-1,1,5,6-tetramethylnaphthalen-2-ol (compound 20) can be selected as the most efficient anti-TB halimane diterpenoids in the series. The different energy parameters of the ligand 20-enzyme Mtb bond in each of the crystal structures are presented in **Table 2**. To analyze the electrostatic effect of the ligand, the ligand of compound 20 and every one of the Mtb enzymes proteins was generated using Discovery Studio Visualizer software [57].

Table 2. Energy value of the binding affinity of each enzyme with each compound and ligand.

Molecules	Binding Affinity against 8F5V (Kcal/mol)	Binding Affinity against 8F2L (Kcal/mol)
1	-7.6	-7.2
2	-7.2	-6.8
3	-6.9	-7.6
4	-6.5	-7
5	-6.9	-7.1
6	-6.8	-7.2
7	-7.2	-7.3
8	-6.9	-7.5
9	-6.5	-7.2
10	-7.1	-7
11	-7.3	-7
12	-6.9	-7
13	-6.9	-6.8
14	-7.3	-6.7

Continued

15	-6.9	-7.7
16	-7.6	-7.1
17	-6.8	-6.8
18	-7	-7
19	-7.1	-7.3
20	-7.6	-8.1
21	-7.6	-7.5
22	-6.9	-7.2
23	-6.6	-6.7
24	-6.7	-7
25	-7.3	-6.3
26	-7.2	-6.6
27	-6.9	-6.6
28	-7	-6.9
29	-6.3	-6.2
30	-6.5	-7.4
31	-8.5	-6.8
32	-6.7	-7.5
33	-7.9	-6.9
34	-7.1	-7.6
35	-7.4	-7.9
36	-7.1	-7.7
37	-7.3	-7.5
38	-7	-6.7
39	-7.1	-6.6
40	-6.7	-6.5
41	-7.1	-6.7
42	-6.7	-7
Natural ligand	-6.6	-4.1

In **Figure 1**, 2D graph shows the various molecular interactions between ligand compound 20, the best potential anti-TB drug, and each of the target enzymatic proteins.

1) Interaction with Mycothiol S-transferase enzyme

Figure 1(a) shows three dark green circles, each connected to a dotted line of the same colour, representing the three conventional hydrogen bonds formed between:

a) The oxygen atom of the terminal hydroxide group of the 5-hydroxy-3-me-

thylpent-3-enyl substituent bonded to carbon 5 of the naphthalene ring and an acceptor hydrogen atom of the X (N or O)-H bond of THR 89;

b) The hydrogen atom of the hydroxide group of the same substituent and a donor atom of the X (N or O) -H bond of THR 89;

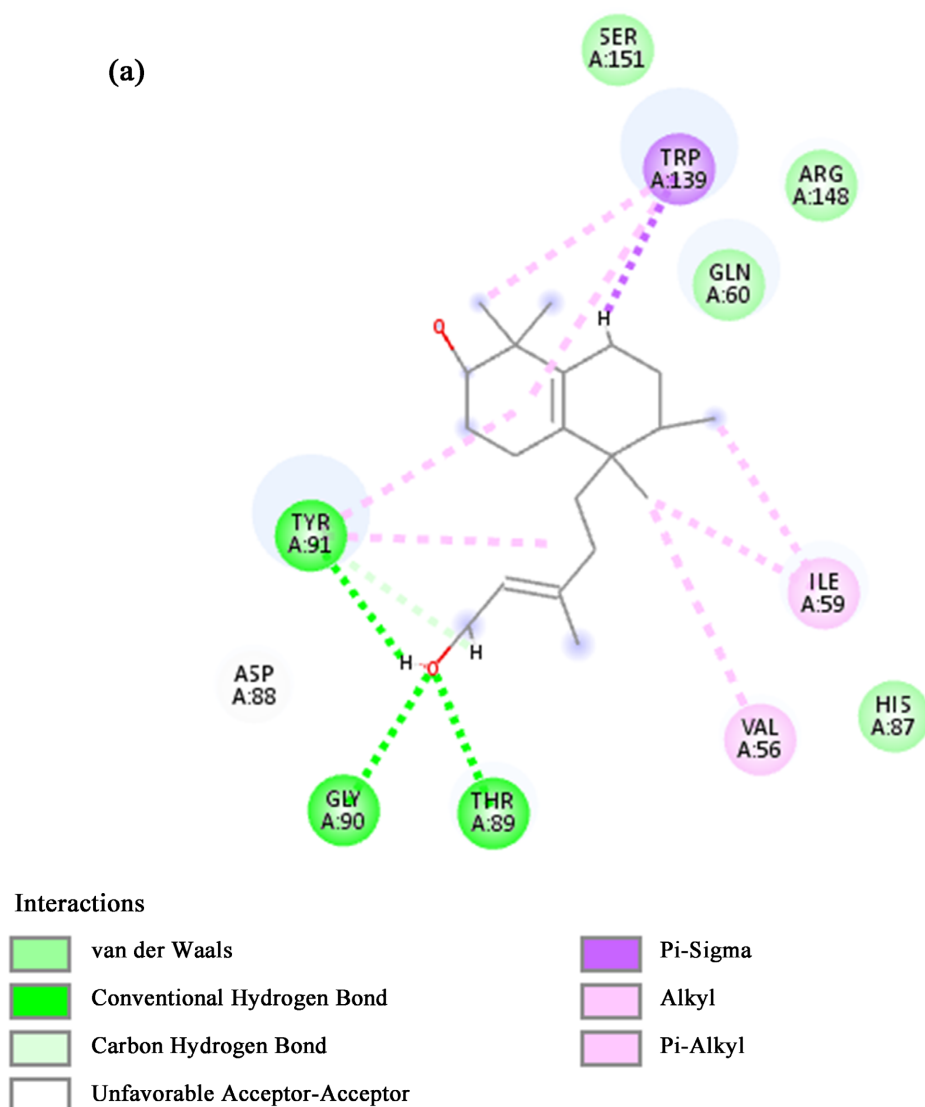
c) The hydrogen atom of this terminal group of the same substituent bonded to carbon 5 of the naphthalene ring and a donor atom of the X (N or O) -H bond of TYP 91. An analysis of the interaction of ligand 20 with Mtb revealed pi-sigma bonds with the acid TRP 139 (purple color).

Additionally, the dark purple indicates the interaction of the Pi-sigma bond with the amino acid TRP 139, which also forms alkyl and pi-alkyl bonds shown in light purple. The amino acids THR 91, VAL 56 and ILE 59 are also colored in the same way.

2) Interaction with Homoserine transacetylase enzyme

In **Figure 1(b)**, the three conventional hydrogen bonds formed are materialized by:

(a)



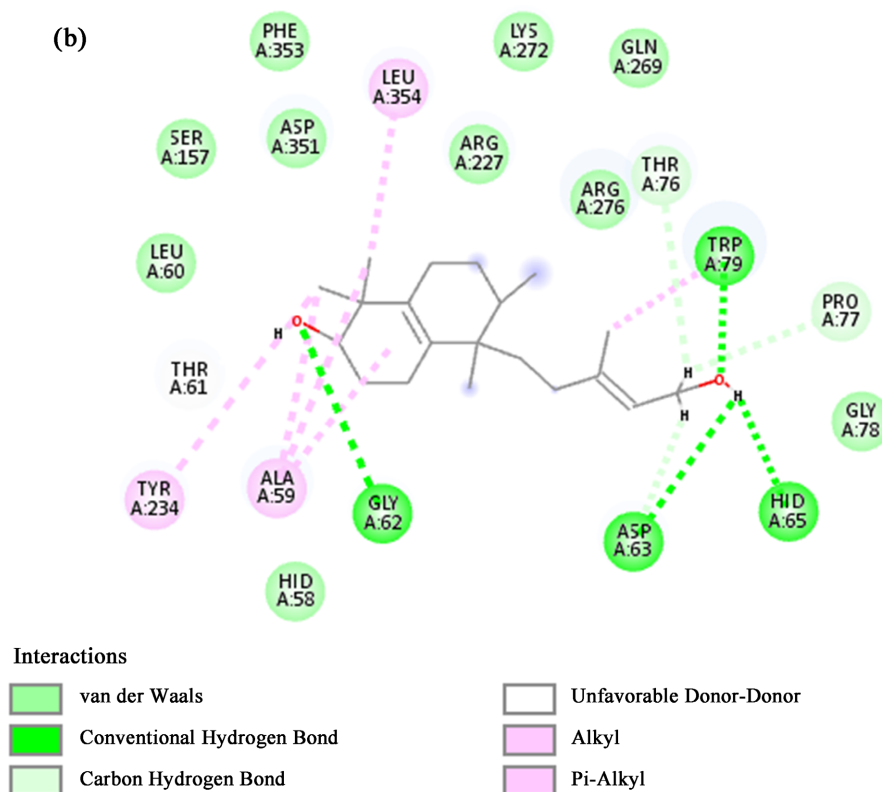


Figure 1. Interaction diagram of (2R,5R,6S)-1,2,3,4,5,6,7,8-octahydro-5-((E)-5-hydroxy-3-methylpent-3-enyl)-1,1,5,6-tetramethylnaphthalen-2-ol with Mycothiol S-transferase enzyme (a) and Homoserine transacetylase enzyme (b).

a) The hydrogen atom of the hydroxide group of the 5-hydroxy-3-methylpent-3-enyl substituent bonded to carbon 5 of the naphthalene ring and a donor atom of the X (N or O)-H bond of PRO 77;

b) The oxygen atom of the hydroxide group bonded to carbon 2 and an acceptor hydrogen atom of the X (N or O)-H bond of GLY 62;

c) The hydrogen atom of the same group bonded to carbon 2 of the naphthalene ring (**Figure 2(b)**) and a donor atom of the X (N or O) -H bond of THR 61. The final oxygen atom of the substituent 5-hydroxy-3-methylpent-3-enyl connected to carbon 5 of the naphthalene ring and the amino acid TRP 79 also form a carbon-hydrogen bond.

The amino acids contributing to the pi-alkyl and alkyl bonds formation are as for ALA 59: three, and one each for LEU 354, TYR 234 and TRP 79.

3.2. Results of Modelling and Optimization Structures

Evaluation of the chemical library's molecules by kinetic stability and chemical reactivity requires analysis of the HOMO-LUMO gap presented in **Table 3**. This descriptor provides a measure of the energies of electronic interactions between orbitals. During the interactions, the frontier orbitals can be electron acceptors for the high altitude electronically unoccupied or electron donors for the low altitude electronically occupied orbitals [58]. A molecule with a high HOMO-LUMO energy

gap has low chemical reactivity and high kinetic stability [59]. Compounds considered unstable and highly reactive have a low HOMO-LUMO energy gap.

In **Table 3**, we show the comparison between the HOMO-LUMO energy gap in gas and water. In gas, the orbitals energies are 6.855 eV. The electronic transition from the HOMO frontier orbital to its LUMO counterpart in this absolute configuration of this compound proves to be therefore very difficult. In aqueous media, there is an average decrease of 1983 eV compared with gaseous media. This decrease in the energies of the frontier orbitals is due to the solvation effect claimed by De Proft and Geerlings [60] [61].

A more extensive kinetic assessment of stability through the different global reactivity descriptors (electronegativity χ , global hardness (η), global softness (S), and electrophilicity index (ω)) was also performed.

The information on the resistance to electron change by a deformation of the electron cloud caused by a small disturbance from the chemical reaction is found from the hardness (η). The selection of the most kinetically stable compound is made according to the criterion of the highest hardness. The average achieved hardness difference is equal to 1585 eV. Our results prove that solvation in water significantly decreases the hardness of the studied molecules. This reduction in hardness values occasioned by the solvation of neutral molecules has been claimed earlier by De Proft and Geerlings [61]. We have measured the deterioration in binding energy due to maximum electron flow between a donor and an acceptor using the overall electrophilicity index (ω). This descriptor, through the measurement of the capacity of a system to gain an electron, enables the prediction of the chemical reactivity of the compound. In gas phase, the highest electrophilicity index is 1.460 for 2.393 in water. The compounds in aqueous solution show that solvation enhances the reactivity. A correlation between the change in the global reactivity descriptor and the solvation energy observed by Parr *et al.* in the framework of the reaction field theory has been confirmed [62].

3.3. Pharmacokinetic and Drug-Likeness Study

Drug-likeness refers to the prediction of whether a specific compound can be developed into a drug. In order to determine drug-likeness, various physiochemical properties of the compound are analyzed using established rules and properties [63].

In 1997, Lipinski and colleagues established the “rule of five”, a filter commonly used to determine whether a molecule is likely to be absorbed orally. According to this rule, to be considered absorbable, a molecule must not exceed

Table 3. HOMO-LUMO gap, electronegativity χ , global hardness (η), global softness (S), and electrophilicity index (ω) in eV of some compounds of halimane diterpenoids.

Molecules	Gas phase					Water				
	HOMO-LUMO gap	χ (eV)	η (eV)	s	ω (eV)	HOMO-LUMO gap	χ (eV)	H (eV)	s	ω (eV)
20	6.855	3.427	4.021	0.124	1.46	4.872	3.414	2.436	0.205	2.393

a certain molecular weight (500 Da), octanol/water partition coefficient (5), number of hydrogen bond donors (5), and number of hydrogen bond acceptors (10) [64]. The Egan filter proposes a maximum lipophilicity (5.88) and total polar surface area (131) for optimal oral bioavailability [65]. Veber and colleagues suggest a maximum number of rotating bonds (10) and total polar surface area (140) for good oral bioavailability [66]. Muegge and his team established criteria including molecular weight (200 - 600), lipophilicity (between -2 and -5), total polar surface area (≤ 150), number of rings (≤ 7), number of carbons (> 4), number of heteroatoms (> 1), number of rotatable bonds (≤ 15), hydrogen bond acceptors (≤ 10), and hydrogen bond donors (≤ 5) [67]. The pharmacokinetic study was based on prediction of blood-brain barrier (BBB) crossing with criterion values (between -3.0 and 1.2), prediction of Caco-2 permeability (< 25 low and > 500 high), percentage oral absorption in humans with values 1, 2, or 3 for low, medium, or high, skin permeability (-8.0 to -1.0) [68]. According to the results of the analysis in **Table 4**, compound 20 has appropriate physicochemical parameters to be considered as a drug crossing the brain barrier (BBB).

Compounds derived from therapeutic treatment of TB meet the criteria for drug eligibility. Compound 20 also shows good results. With regard to Human Oral Absorption (HOA), which is strongly recommended by the WHO as an absorption criterion, compound 20 has good absorption potential. It is more effective at passively crossing the intestinal permeability barrier than first-line treatments (ethambutol, isoniazid).

3.4. Molecular Dynamic Simulation Results

Molecular dynamics simulation (MDs) is an essential computational tool for understanding the physical and chemical properties of drug candidate compounds. It is seen as a study of relative positional changes of a moving molecule system in a protein over time [69].

MDs first bring to life biomolecular structures in solution at different timelines, giving a view of natural dynamics. Secondly, it allows us to find values for several molecular properties as close as possible to experimental data. Finally, it explores the different conformations of molecular structures in space [70].

Table 4. Assessment of the pharmacokinetic profiles of compound 20 and anti-TB drugs therapy (ethambutol Isoniazid and amikacin), using the recommended screening for 95% of known drugs.

Molecules	MW	QPlog-Po/w	^d QPlogPw	HBA	HBD	QPlog BB	QPPCaco	Volume	#rotor	QPlogK _{hsa}	QPlog HERG	QPlog K _p	PSA	Human-Oral Absorption
Compound 20	306.5	3.964	6.821	3.4	2.000	-0.636	1253.6	1105.062	6	0.642	-3.723	-3.05	49.813	3
ethambutol	204.312	-0.232	11.357	6.400	4.000	-0.241	66.852	830.487	0	-0.785	-5.413	-6.463	63.513	2
isoniazid	137.141	-0.649	11.122	4.500	3.000	-0.838	275.982	495.524	0	-0.755	-3.543	-3.773	81.402	2
amikacin.	585.607	-8.352	53.383	26.900	17.000	-4.341	0.004	1549.406	1	-2.258	-5.699	-12.007	322.557	1

Our study will examine the stability of docking-validated complexes to see how they perform in MDs.

The Root Mean Square Deviation (RMSD) serves as a metric for evaluating the stability of a system. Specifically, it measures the average displacement of a set of atoms relative to a reference frame. For globular and small proteins, the permissible range of structural conformations falls between 1 and 31. The RMSD evolution between the Mtb Homoserine transacetylase and the ligand (compound 20) is depicted in **Figure 2(a)**. Between 0 and 40 nsec, the Lig fit Prot curve is far from the reference protein scaffold, suggesting instability within the complex. However, from 40 to 60 nsec, there is an alignment with the reference protein backbone, indicating structural stability. Beyond 60 nsec, there is an RMSD deviation as a function of time, indicating instability of ligand-protein conformations. In contrast, **Figure 3(a)** illustrates the stable structural conformation of the ligand and the atoms of the reference protein Mycothiol S-transferase enzyme. Although there is a sudden shift away from each other between 55 and 90 nsec, reflecting instability of the complex, the two structures converge once more in the last 10 nsec. Both complexes exhibit an RMSD of less than 3.0 Å, indicating their stability.

In accordance with the analysis of the protein-RMSF graph, the RMSF value proves to be a useful tool for assessing the fluctuations of residues in molecular dynamics simulations. It is particularly beneficial in evaluating the quality of amino acid binding at a binding site. RMSF values that are high suggest suboptimal binding. Upon examining the protein-RMSF plot depicted in **Figure 2(b)**, it is apparent that the interaction between the compound 20 and the protein's residue, as indicated by the green lines, is stable, with values below 1.8 Å. Conversely, residue fluctuation values on the protein that are greater than 2 Å suggest a weak interaction between the ligand and the protein. **Figure 3(b)** also illustrates the stability of the compound 20 and residue, although the RMSF value is 2.2 Å, which is below the cut-off value of 2.5 (vita). However, all protein-mediated fluctuations remain below 2 Å, indicating a strong interaction.

According to **Figure 2(c)** show the protein amino acids that interact with the ligand. Therefore, we have THR 61, SER 157 and HIS 350 for hydrogen bonds. The amino acids involved in hydrophilic interactions are as follows: ALA 59, LEU 60, ALA 230 TYR 234, TYR 282, LEU 289, LEU 322, PHE 353 and LEU 354. We have selected ALA 59, LEU 60, THR 61, ASP 63, HIS 65, THR 76, PRO 77, SER157, ARG 227 and ASP 351 for protein-ligand interactions with hydrogen in water (water bridges). For **Figure 3(c)**, hydrogen bonds are established between GLN 60, HIS 87, ASP 88, THR 89, TYR 91, TRP 139, ASN 140, SER 151, ASP 154 and ASP 155. In terms of hydrophobic bonds, the ligand interacts with VAL 56, ILE 59, TYR 91, TRP 139, ASN 140, PRO 141 and ILE 152. Atoms of the ligand and the acids HIS 52, GLN 60, ARG 86, HIS 87, ASP 88, THR 89, GLY 90, TYR 91, SER 138, TRP 139, ASN 140, PRO 141, ALA 147, ARG 148, SER 151, ASP 154 and ASP 155 form water bridges. The ligand and ASN 140 bond in polar mode.

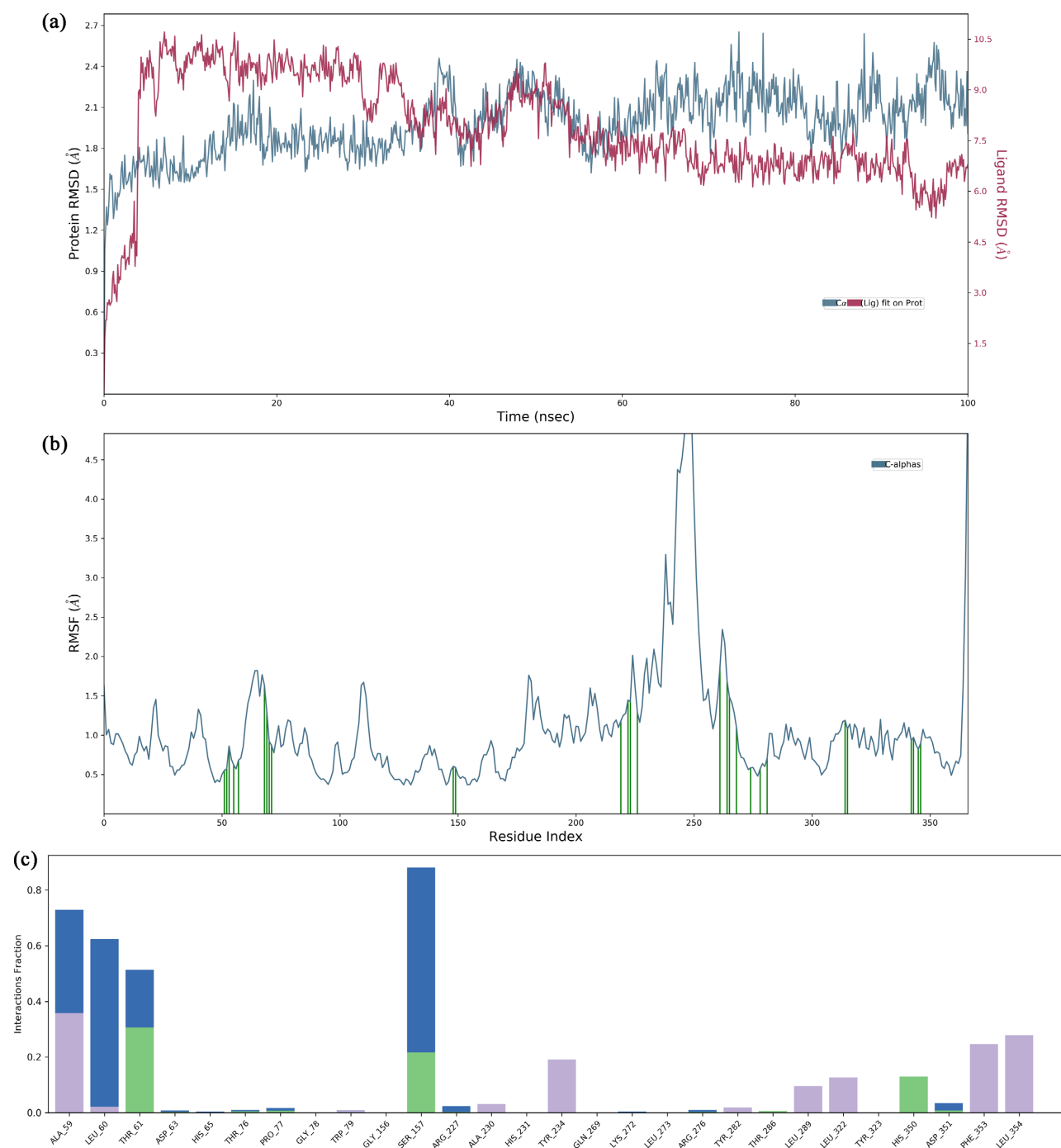


Figure 2. Simulation Interactions graphs of compound 20 (ligand 8F2L (protein)): (a) Protein-Ligand RMSD; (b) Protein RMSF. (c) Protein-Ligand Contacts.

3.5. Interaction Energy Calculations

The study of the non-bonded interactions between each residue of the receptor and the small molecule revealed the individual contribution of each residue to the total interaction energy. This was done by calculating the sum of the van der Waals and electrostatic interaction energies of each residue. This analysis allowed us to understand the role of each residue in binding to the small molecule.

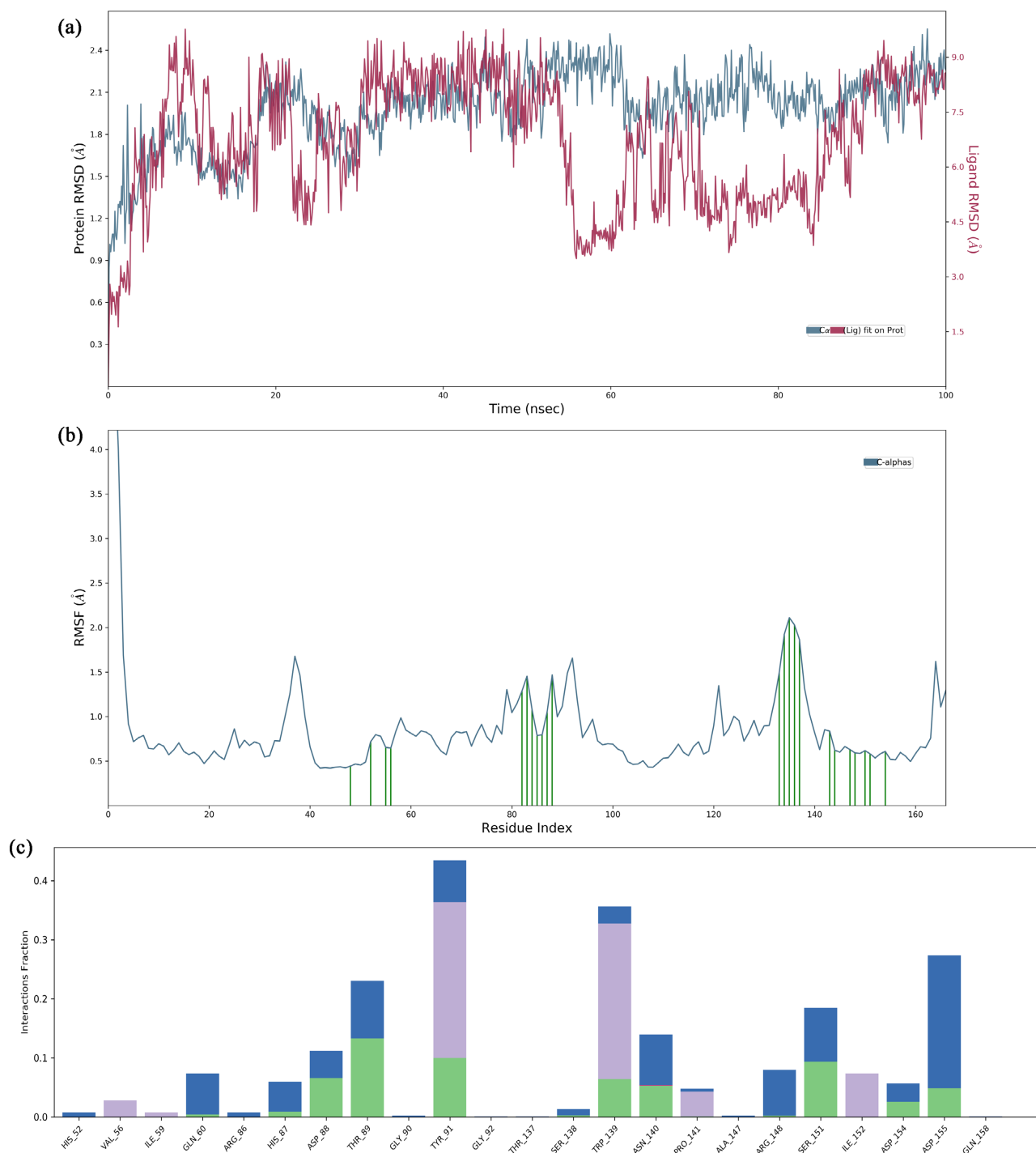


Figure 3. Simulation Interactions graphs of compound 20 (ligand) –8F5V (protein): (a) Protein-Ligand RMSD. (b) Protein RMSF. (c) Protein-Ligand Contacts.

Several residues showed lower interaction energy values ranging from 0 to -12.0 kcal/mol. The results allow us to rank our residues in descending order according to their protein-ligand interaction stability: THR 89, GLY 90, ARG 148, VAL 56, GLN 60. This compensated for the perturbing contribution energies of residues such as ILE 59, HIS 87 and ASP 88 whose total energy was greater than.

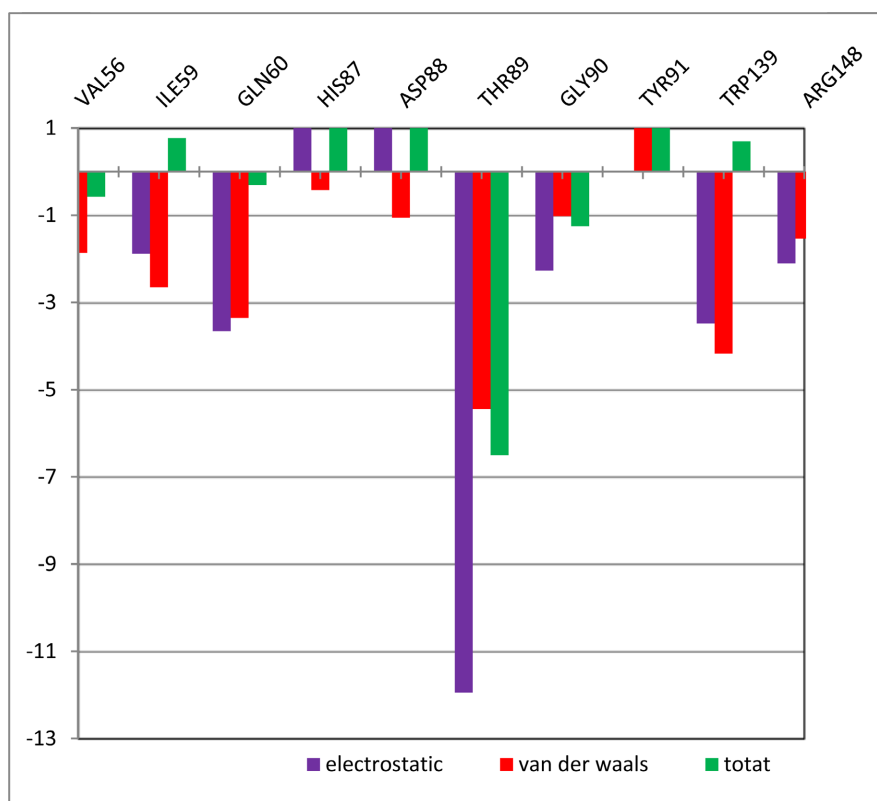


Figure 4. Interaction energies (electrostatic, van der waals, total) of some residues of Mycothiol S-transferase enzyme and ligand.

4. Conclusion

Evaluation of the molecules in our chemical library by molecular docking shows that (2R,5R,6S)-1,2,3,4,5,6,7,8-octahydro-5-((E)-5-hydroxy-3-methylpent-3-enyl)-1,1,5,6-tetramethylnaphthalene-2-ol is the best ligand for binding affinity with the Mtb Mycothiol S-transferase and Mtb Homoserine transacetylase enzymes, respectively. Molecular dynamics simulations reveal that the interaction between the crystalline structure of the Mtb Mycothiol S-transferase enzyme and is the most effective over time. Analysis of kinetic stability and chemical reactivity through the HOMO-LUMO gap study shows good stability of the compound with excellent stability of the series in both media. For pharmacokinetic requirements, our molecule meets all the criteria. Further studies can be carried out, such as *in vitro* and *in vivo* evaluations are recommended.

Acknowledgements

The author is immensely grateful to Prof. Dr. Fidele Ntie-Kang for his technical assistance during this work.

Author Contributions

Conceptualization, B.D.B. and B.M.D.; methodology, E.A.L.G., B.D.B., B.M.D., P.A.O., and M.M.L.L.; writing-original draft preparation: E.A.L.G. and B.D.B.;

writing-review and editing: B.M.D. L.C.O.O. and M.M.L.L. All authors have read and agreed to the published version of the manuscript.

Statement of Usage of Artificial Intelligence

Not applicable.

Data Availability Statement

Not applicable.

Funding Information

Not applicable.

Conflicts of Interest

The authors declare no conflicts of interest regarding the publication of this paper.

References

- [1] Dye, C., Harries, A.D., Maher, D., Hosseini, S.M., Nkhoma, W. and Salaniponi, F.M. (2006) Tuberculosis. In: Jamison, D.T., Feachem, R.G., Makgoba, M.W., Bos, E.R., Baingana, F.K., Hofman, K.J. and Rogo, K.O., Eds., *Disease and Mortality in Sub-Saharan Africa (2nd Edition)*, The International Bank for Reconstruction and Development, The World Bank, Washington DC, 179-195.
<http://www.ncbi.nlm.nih.gov/books/NBK2285/>
- [2] Adebisi, Y.A., Agumage, I., Sylvanus, T.D., Nawaila, I.J., Ekwere, W.A., Nasiru, M., Okon, E.E., Ekpenyong, A.M. and Iii, D.E.L.P. (2019) Burden of Tuberculosis and Challenges Facing Its Eradication in West Africa. *International Journal of Infection*, **6**, e92250. <https://doi.org/10.5812/iji.92250>
- [3] Atanasov, A.G., Zotchev, S.B., Dirsch, V.M. and Supuran, C.T. (2021) Natural Products in Drug Discovery: Advances and Opportunities. *Nature Reviews Drug Discovery*, **20**, 200-216. <https://doi.org/10.1038/s41573-020-00114-z>
- [4] Mahesh, G., Kumar, K.A. and Reddanna, P. (2021) Overview on the Discovery and Development of Anti-Inflammatory Drugs: Should the Focus Be on Synthesis or Degradation of PGE₂? *Journal of Inflammation Research*, **14**, 253-263.
<https://doi.org/10.2147/JIR.S278514>
- [5] Knowles, R.G. (2014) Development of Anti-Inflammatory Drugs—The Research and Development Process. *Basic & Clinical Pharmacology & Toxicology*, **114**, 7-12.
<https://doi.org/10.1111/bcpt.12130>
- [6] Ramos-Martín, F. and D'Amelio, N. (2023) Drug Resistance: An Incessant Fight against Evolutionary Strategies of Survival. *Microbiology Research*, **14**, 507-542.
<https://doi.org/10.3390/microbiolres14020037>
- [7] Halawa, E.M., Fadel, M., Al-Rabia, M.W., Abdo, M., Atwa, A.M. and Abdeen, A. (2024) Antibiotic Action and Resistance: Updated Review of Mechanisms, Spread, Influencing Factors, and Alternative Approaches for Combating Resistance. *Frontiers in Pharmacology*, **14**, Article 1305294.
<https://doi.org/10.3389/fphar.2023.1305294>
- [8] Grinter, S.Z. and Zou, X. (2014) Challenges, Applications, and Recent Advances of

- Protein-Ligand Docking in Structure-Based Drug Design. *Molecules*, **19**, 10150-10176. <https://doi.org/10.3390/molecules190710150>
- [9] Rica, E., Álvarez, S. and Serratos, F. (2021) Ligand-Based Virtual Screening Based on the Graph Edit Distance. *International Journal of Molecular Sciences*, **22**, Article 12751. <https://doi.org/10.3390/ijms222312751>
- [10] Seid, A., Girma, Y., Abebe, A., Dereb, E., Kassa, M. and Berhane, N. (2023) Characteristics of TB/HIV Co-Infection and Patterns of Multidrug-Resistance Tuberculosis in the Northwest Amhara, Ethiopia. *Infection and Drug Resistance*, **16**, 3829-3845. <https://doi.org/10.2147/IDR.S412951>
- [11] Bhatt, A., Quazi Syed, Z. and Singh, H. (2023) Converging Epidemics: A Narrative Review of Tuberculosis (TB) and Human Immunodeficiency Virus (HIV) Coinfection. *Cureus*, **15**, e47624.
- [12] Sultana, Z.Z., Hoque, F.U., Beyene, J., Akhlak-Ul-Islam, M., Khan, M.H.R., Ahmed, S., Hawlader, D.H. and Hossain, A. (2021) HIV Infection and Multidrug Resistant Tuberculosis: A Systematic Review and Meta-Analysis. *BMC Infectious Diseases*, **21**, Article No. 51. <https://doi.org/10.1186/s12879-020-05749-2>
- [13] Cruz-Knight, W. and Blake-Gumbs, L. (2013) Tuberculosis. *Primary Care: Clinics in Office Practice*, **40**, 743-756. <https://doi.org/10.1016/j.pop.2013.06.003>
- [14] Bagcchi, S. (2023) WHO's Global Tuberculosis Report 2022. *The Lancet Microbe*, **4**, E20. [https://doi.org/10.1016/S2666-5247\(22\)00359-7](https://doi.org/10.1016/S2666-5247(22)00359-7)
- [15] Shastri, M.D., Shukla, S.D., Chong, W.C., Dua, K., Peterson, G.M., Patel, R.P., Hansbro, P.M., Eri, R. and O'Toole, R.F. (2018) Role of Oxidative Stress in the Pathology and Management of Human Tuberculosis. *Oxidative Medicine and Cellular Longevity*, **2018**, Article ID: 7695364. <https://doi.org/10.1155/2018/7695364>
- [16] Carr, W. (2022) Interim Guidance: 4-Month Rifapentine-Moxifloxacin Regimen for the Treatment of Drug-Susceptible Pulmonary Tuberculosis—United States, 2022. *Morbidity and Mortality Weekly Report*, **71**, 285-289. <https://doi.org/10.15585/mmwr.mm7108a1>
- [17] Nahid, P., Dorman, S.E., Alipanah, N., Barry, P.M., Brozek, J.L., Cattamanchi, A., Chaisson, L.H., Chaisson, R.E., Daley, C.L., Grzemska, M., Higashi, J.M., Ho, C.S., Hopewell, P.C., Keshavjee, S.A., Lienhardt, C., Menzies, R., Merrifield, C., Narita, M., O'Brien, R., Vernon, A., *et al.* (2016) Executive Summary: Official American Thoracic Society/Centers for Disease Control and Prevention/Infectious Diseases Society of America Clinical Practice Guidelines: Treatment of Drug-Susceptible Tuberculosis. *Clinical Infectious Diseases*, **63**, 853-867. <https://doi.org/10.1093/cid/ciw566>
- [18] Shin, H.J. and Kwon, Y.S. (2015) Treatment of Drug Susceptible Pulmonary Tuberculosis. *Tuberculosis and Respiratory Diseases*, **78**, 161-167. <https://doi.org/10.4046/trd.2015.78.3.161>
- [19] Chakaya, J., Khan, M., Ntoumi, F., Aklilu, E., Fatima, R., Mwaba, P., Kapata, N., Mfinanga, S., Hasnain, S.E., Katoto, P.D.M.C., Bulabula, A.N.H., Sam-Agudu, N.A., Nachega, J.B., Tiberi, S., McHugh, T.D., Abubakar, I. and Zumla, A. (2021) Global Tuberculosis Report 2020—Reflections on the Global TB Burden, Treatment and Prevention Efforts. *International Journal of Infectious Diseases*, **113**, S7-S12. <https://doi.org/10.1016/j.ijid.2021.02.107>
- [20] Khameneh, B., Fazly Bazzaz, B.S., Amani, A., Rostami, J. and Vahdati-Mashhadian, N. (2016) Combination of Anti-Tuberculosis Drugs with Vitamin C or NAC against Different *Staphylococcus aureus* and *Mycobacterium tuberculosis* Strains. *Microbial Pathogenesis*, **93**, 83-87. <https://doi.org/10.1016/j.micpath.2015.11.006>

- [21] Roncero, A.M., Tobal, I.E., Moro, R.F., Díez, D. and Marcos, I.S. (2018) Halimane Diterpenoids: Sources, Structures, Nomenclature and Biological Activities. *Natural Product Reports*, **35**, 955-991. <https://doi.org/10.1039/C8NP00016F>
- [22] Okerio, K.N., Kenanda, E.O. and Omosa, L.K. (2019) Antiproliferative Properties of Labdane Diterpenoids from *Croton Sylvaticus* Hochst against Drug Sensitive and Resistant Leukemia Cell Lines. *Investigational Medicinal Chemistry and Pharmacology*, **2**, 1-5. <https://doi.org/10.31183/imcp.2019.00031>
- [23] Maroyi, A. (2017) Traditional Usage, Phytochemistry and Pharmacology of *Croton sylvaticus* Hochst. Ex C. Krauss. *Asian Pacific Journal of Tropical Medicine*, **10**, 423-429. <https://doi.org/10.1016/j.apjtm.2017.05.002>
- [24] Stafford, G.I., Pedersen, P.D., Jäger, A.K. and Van Staden, J. (2007) Monoamine Oxidase Inhibition by Southern African Traditional Medicinal Plants. *South African Journal of Botany*, **73**, 384-390. <https://doi.org/10.1016/j.sajb.2007.03.001>
- [25] Hoshino, T., Nakano, C., Ootsuka, T., Shinohara, Y. and Hara, T. (2010) Substrate Specificity of Rv3378c, an Enzyme from *Mycobacterium tuberculosis*, and the iNhibitory Activity of the Bicyclic Diterpenoids against Macrophagephagocytosis. *Organic & Biomolecular Chemistry*, **9**, 2156-2165. <https://doi.org/10.1039/C0OB00884B>
- [26] Mangel, N., Mann, F.M., Hillwig, M.L., Peters, R.J. and Snider, B.B. (2010) Synthesis of (±)-Nosyberkol (Isotuberculosinol, Revised Structure of Edaxadiene) and (±)-Tuberculosinol. *Organic Letters*, **12**, 2626-2629. <https://doi.org/10.1021/ol100832h>
- [27] Soudani, W., Hadjadj-Aoul, F.Z., Bouachrine, M. and Zaki, H. (2021) Molecular Docking of Potential Cytotoxic Alkylating Carmustine Derivatives 2-Chloroethylnitrososulfamides Analogues of 2-Chloroethylnitrosoureas. *Journal of Biomolecular Structure and Dynamics*, **39**, 4256-4269. <https://doi.org/10.1080/07391102.2020.1776638>
- [28] Jayasinghe, Y.P., Banco, M.T., Lindenberger, J.J., Favrot, L., Palčeková, Z., Jackson, M., Manabe, S. and Ronning, D.R. (2023) The *Mycobacterium tuberculosis* Mycothiol S-Transferase Is Divalent Metal-Dependent for Mycothiol Binding and Transfer. *RSC Medicinal Chemistry*, **14**, 491-500. <https://doi.org/10.1039/D2MD00401A>
- [29] Sharma, S., Jayasinghe, Y.P., Mishra, N.K., Orimoloye, M.O., Wong, T.Y., Dalluge, J.J., Ronning, D.R. and Aldrich, C.C. (2023) Structural and Functional Characterization of *Mycobacterium tuberculosis* Homoserine Transacetylase. *ACS Infectious Diseases*, **9**, 540-553. <https://doi.org/10.1021/acsinfecdis.2c00541>
- [30] Darmadi, D., Lindarto, D., Siregar, J., Widyawati, T., Rusda, M., Amin, M.M., Yusuf, F., Eyanoe, P.C., Lubis, M. and Rey, I. (2023) Study of the Molecular Dynamics Stability in the Inhibitory Interaction of Tenofovir Disoproxil Fumarate against CTLA-4 in Chronic Hepatitis B Patients. *Medical Archives*, **77**, 227-230. <https://doi.org/10.5455/medarh.2023.77.227-230>
- [31] Ounthaisong, U. and Tangyuenyongwatana, P. (2017) Cross-Docking Study of Flavonoids against Tyrosinase Enzymes Using PyRx 0.8 Virtual Screening Tool. <https://www.researchgate.net/publication/316546901>
- [32] Morris, G.M. and Lim-Wilby, M. (2008) Molecular Docking. In: Kukol, A., Ed., *Methods in Molecular Biology*, Humana Press, Clifton, 365-382. https://doi.org/10.1007/978-1-59745-177-2_19
- [33] Prieto-Martínez, F.D., Arciniega, M. and Medina-Franco, J.L. (n.d.) Molecular Docking: Current Advances and Challenges. *TIP. Revista Especializada En Ciencias*

- Químico-Biológicas*, **21**, 1-24.
- [34] Kumar, S.A. and Bhaskar, B.L. (2019) Computational and Spectral Studies of 3,3'-(Propane-1,3-Diyl) Bis (7,8-Dimethoxy-1,3,4, 5-Tetrahydro-2H-Benzo[d]Azepin-2-one). *Heliyon*, **5**, e02420. <https://doi.org/10.1016/j.heliyon.2019.e02420>
 - [35] Sethi, A., Joshi, K., Sasikala, K. and Alvala, M. (2020) Molecular Docking in Modern Drug Discovery: Principles and Recent Applications. In: Gaitonde, V., Karmakar, P. and Trivedi, A., Eds., *Drug Discovery and Development—New Advances*, IntechOpen, Hong Kong, China, 1-21. <https://doi.org/10.5772/intechopen.85991>
 - [36] Becke, A.D. (1988) Density-Functional Exchange-Energy Approximation with Correct Asymptotic Behavior. *Physical Review A*, **38**, 3098-3100. <https://doi.org/10.1103/PhysRevA.38.3098>
 - [37] Lee, C., Yang, W. and Parr, R.G. (1988) Development of the Colle-Salvetti Correlation-Energy Formula into a Functional of the Electron Density. *Physical Review B, Condensed Matter*, **37**, 785-789. <https://doi.org/10.1103/PhysRevB.37.785>
 - [38] Matin, M.A., Bhattacharjee, S., Shaikh, M.A.A., Debnath, T. and Aziz, M.A. (2020) A Density Functional Theory (DFT) Investigation on the Structure and Spectroscopic Behavior of 2-Aminoterephthalic Acid and Its Sodium Salts. *Green and Sustainable Chemistry*, **10**, 39-55. <https://doi.org/10.4236/gsc.2020.102004>
 - [39] Sheela, N., Muthu, S. and Sampathkrishnan, S. (2013) Molecular Orbital Studies (Hardness, Chemical Potential and Electrophilicity), Vibrational Investigation and Theoretical NBO Analysis of 4-4'-(1H-1, 2, 4-Triazol-1-yl Methylene) Dibenzonitrile Based on Abinitio and DFT Methods. *Spectrochimica Acta Part A: Molecular and Biomolecular Spectroscopy*, **120**, 237-251. <https://doi.org/10.1016/j.saa.2013.10.007>
 - [40] De la Vega, J.G. and Miguel, B. (2003) Basis Sets for Computational Chemistry. In: Montero, L.A., Diaz, L.A. and Bader, R., Eds., *Introduction to Advanced Topics of Computational Chemistry*, Citeseer, Havana, 41-80.
 - [41] Shivanika, C., et al. (2022) Molecular Docking, Validation, Dynamics Simulations, and Pharmacokinetic Prediction of Natural Compounds against the SARS-CoV-2 Main-Protease. *Journal of Biomolecular Structure & Dynamics*, **40**, 585-611.
 - [42] Liu, H., Jin, Y. and Ding, H. (2023) MDBuilder: A PyMOL Plugin for the Preparation of Molecular Dynamics Simulations. *Briefings in Bioinformatics*, **24**, bbad057. <https://doi.org/10.1093/bib/bbad057>
 - [43] El Aissouq, A., Chedadi, O., Bouachrine, M. and Ouammou, A. (2021) Identification of Novel SARS-CoV-2 Inhibitors: A Structure-Based Virtual Screening Approach. *Journal of Chemistry*, **2021**, Article ID: 1901484. <https://doi.org/10.1155/2021/1901484>
 - [44] Guan, L., Yang, H., Cai, Y., Sun, L., Di, P., Li, W., Liu, G. and Tang, Y. (2018) ADMET-Score—A Comprehensive Scoring Function for Evaluation of Chemical Drug-Likeness. *MedChemComm*, **10**, 1-11. <https://doi.org/10.1039/C8MD00472B>
 - [45] Baldi, A. (2010) Computational Approaches for Drug Design and Discovery: An Overview. *Systematic Reviews in Pharmacy*, **1**, 99. <https://doi.org/10.4103/0975-8453.59519>
 - [46] Flores-Holguín, N., Frau, J. and Glossman-Mitnik, D. (2021) Computational Pharmacokinetics Report, ADMET Study and Conceptual DFT-Based Estimation of the Chemical Reactivity Properties of Marine Cyclopeptides. *ChemistryOpen*, **10**, 1142-1149. <https://doi.org/10.1002/open.202100178>
 - [47] Moto Ongagna, J., Tamafo Fouegue, A.D., Ateba Amana, B., Mouzong D'ambassa, G., Zobo Mfomo, J., Mbaze Meva'A, L. and Bikele Mama, D. (2020) B3LYP, M06

- and B3PW91 DFT Assignment of nd8 Metal-Bis-(N-Heterocyclic Carbene) Complexes. *Journal of Molecular Modeling*, **26**, Article No. 246. <https://doi.org/10.1007/s00894-020-04500-7>
- [48] Bai, G., Pan, Y., Zhang, Y., Li, Y., Wang, J., Wang, Y., Teng, W., Jin, G., Geng, F. and Cao, J. (2023) Research Advances of Molecular Docking and Molecular Dynamic Simulation in Recognizing Interaction between Muscle Proteins and Exogenous Additives. *Food Chemistry*, **429**, Article ID: 136836. <https://doi.org/10.1016/j.foodchem.2023.136836>
- [49] Darden, T., York, D. and Pedersen, L. (1993) Particle Mesh Ewald: An $N \log(N)$ Method for Ewald Sums in Large Systems. *The Journal of Chemical Physics*, **98**, 10089-10092. <https://doi.org/10.1063/1.464397>
- [50] Antonini, G., Civera, M., Lal, K., Mazzotta, S., Varrot, A., Bernardi, A. and Belvisi, L. (2023) Glycomimetic Antagonists of BC2L-C Lectin: Insights from Molecular Dynamics Simulations. *Frontiers in Molecular Biosciences*, **10**, Article 1201630. <https://doi.org/10.3389/fmolb.2023.1201630>
- [51] Braňka, A. (2000) Nosé-Hoover Chain Method for Nonequilibrium Molecular Dynamics Simulation. *Physical Review E*, **61**, 4769-4773. <https://doi.org/10.1103/PhysRevE.61.4769>
- [52] Bekono, B.D., Esmel, A.E., Dali, B., Ntie-Kang, F., Keita, M., Owono, L.C. and Megnassan, E. (2021) Computer-Aided Design of Peptidomimetic Inhibitors of Falcipain-3: QSAR and Pharmacophore Models. *Scientia Pharmaceutica*, **89**, Article 44. <https://doi.org/10.3390/scipharm89040044>
- [53] Bekono, B.D., Sona, A.N., Eni, D.B., Owono, L.C.O., Megnassan, E. and Ntie-Kang, F. (2021) 13 Molecular Mechanics Approaches for Rational Drug Design: Force-fields and Solvation Models. In: Ramasami, P., Ed., *Computational Chemistry: Applications and New Technologies*, De Gruyter, Berlin, 233-254. <https://doi.org/10.1515/9783110682045-013>
- [54] Zhu, X., Lopes, P.E. and Mackerell Jr., A.D. (2012) Recent Developments and Applications of the CHARMM Force Fields. *WIREs Computational Molecular Science*, **2**, 167-185. <https://doi.org/10.1002/wcms.74>
- [55] Rossino, G., Rui, M., Pozzetti, L., Schepmann, D., Wünsch, B., Zampieri, D., Pella-vio, G., Laforenza, U., Rinaldi, S., Colombo, G., Morelli, L., Linciano, P., Rossi, D. and Collina, S. (2020) Setup and Validation of a Reliable Docking Protocol for the Development of Neuroprotective Agents by Targeting the Sigma-1 Receptor (S1R). *International Journal of Molecular Sciences*, **21**, Article 7708. <https://doi.org/10.3390/ijms21207708>
- [56] Wang, Y., Jiao, Q., Wang, J., Cai, X., Zhao, W. and Cui, X. (2023) Prediction of Protein-Ligand Binding Affinity with Deep Learning. *Computational and Structural Biotechnology Journal*, **21**, 5796-5806. <https://doi.org/10.1016/j.csbj.2023.11.009>
- [57] Qasaymeh, R.M., Rotondo, D., Oosthuizen, C.B., Lall, N. and Seidel, V. (2019) Predictive Binding Affinity of Plant-Derived Natural Products towards the Protein Kinase G Enzyme of Mycobacterium tuberculosis (MtPknG). *Plants*, **8**, Article 477. <https://doi.org/10.3390/plants8110477>
- [58] Yonezawa, T., Shingu, H. and Fukui, K. (1952) A Molecular Orbital Theory of Reactivity in Aromatic Hydrocarbons. *The Journal of Chemical Physics*, **50**, 722-725.
- [59] Miar, M., Shiroudi, A., Pourshamsian, K., Oliaey, A.R. and Hatamjafari, F. (2021) Theoretical Investigations on the HOMO–LUMO Gap and Global Reactivity Descriptor Studies, Natural Bond Orbital, and Nucleus-Independent Chemical Shifts Analyses of 3-Phenylbenzo[d]Thiazole-2(3H)-Imine and Its Para-Substituted Deriva-

- tives: Solvent and Substituent Effects. *Journal of Chemical Research*, **45**, 147-158. <https://doi.org/10.1177/1747519820932091>
- [60] Belviso, S., Santoro, E., Lelj, F., Casarini, D., Villani, C., Franzini, R. and Superchi, S. (2018) Stereochemical Stability and Absolute Configuration of Atropisomeric Alkylthioporphyrazines by Dynamic NMR and HPLC Studies and Computational Analysis of HPLC-ECD Recorded Spectra. *European Journal of Organic Chemistry*, **2018**, 4029-4037. <https://doi.org/10.1002/ejoc.201800553>
- [61] Geerlings, P., De Proft, F. and Langenaeker, W. (2003) Conceptual Density Functional Theory. *Chemical Reviews*, **103**, 1793-1874. <https://doi.org/10.1021/cr990029p>
- [62] Parr, R.G., Szentpály, L.V. and Liu, S. (1999) Electrophilicity Index. *Journal of the American Chemical Society*, **121**, 1922-1924. <https://doi.org/10.1021/ja983494x>
- [63] Kralj, S., Jukić, M. and Bren, U. (2023) Molecular Filters in Medicinal Chemistry. *Encyclopedia*, **3**, 501-511. <https://doi.org/10.3390/encyclopedia3020035>
- [64] Lipinski, C.A., Lombardo, F., Dominy, B.W. and Feeney, P.J. (2001) Experimental and Computational Approaches to Estimate Solubility and Permeability in Drug Discovery and Development Settings. *Advanced Drug Delivery Reviews*, **46**, 3-26. [https://doi.org/10.1016/S0169-409X\(00\)00129-0](https://doi.org/10.1016/S0169-409X(00)00129-0)
- [65] Jia, C.Y., Li, J.Y., Hao, G.F. and Yang, G.F. (2020) A Drug-Likeness Toolbox Facilitates ADMET Study in Drug Discovery. *Drug Discovery Today*, **25**, 248-258. <https://doi.org/10.1016/j.drudis.2019.10.014>
- [66] Dobson, P.D. and Kell, D.B. (2008) Carrier-Mediated Cellular Uptake of Pharmaceutical Drugs: An Exception or the Rule? *Nature Reviews Drug Discovery*, **7**, 205-220. <https://doi.org/10.1038/nrd2438>
- [67] Muegge, I., Heald, S.L. and Brittelli, D. (2001) Simple Selection Criteria for Drug-Like Chemical Matter. *Journal of Medicinal Chemistry*, **44**, 1841-1846. <https://doi.org/10.1021/jm015507e>
- [68] Gupta, M., Lee, H.J., Barden, C.J. and Weaver, D.F. (2019) The Blood-Brain Barrier (BBB) Score. *Journal of Medicinal Chemistry*, **62**, 9824-9836. <https://doi.org/10.1021/acs.jmedchem.9b01220>
- [69] Karplus, M. and Petsko, G.A. (1990) Molecular Dynamics Simulations in Biology. *Nature*, **347**, 631-639. <https://doi.org/10.1038/347631a0>
- [70] Hansson, T., Oostenbrink, C. and van Gunsteren, W. (2002) Molecular Dynamics Simulations. *Current Opinion in Structural Biology*, **12**, 190-196. [https://doi.org/10.1016/S0959-440X\(02\)00308-1](https://doi.org/10.1016/S0959-440X(02)00308-1)